TECHNICAL REPORT

INTEGRAL-METHOD ANALYSIS FOR A HYPERSONIC VISCOUS SHOCK LAYER WITH MASS INJECTION

By: Sang-Wook Kang and Michael G. Dunn

CAL No. AI-2187-A-8

Prepared For:

National Aeronautic Space Administration
Goddard Space Flight Center
Greenbelt, Maryland

CAL Report No. AI-2187-A-8
Contract No. NAS5-9978
April 1968

CORNELL AERONAUTICAL LABORATORY, INC.
OF CORNELL UNIVERSITY, BUFFALO, N. Y. 14221

CORNELL AERONAUTICAL LABORATORY, INC.
BUFFALO, NEW YORK 14221

INTEGRAL-METHOD ANALYSIS FOR A HYPERSONIC VISCOUS SHOCK LAYER WITH MASS INJECTION

CAL Report No. AI-2187-A-8

April 1968

PREPARED BY: Sang Wook Kang
Sang-Wook Kang

APPROVED BY: J. Gordon Hall
J. Gordon Hall, Head
Aerodynamic Research Department

Michael G. Dunn
Michael G. Dunn

FOREWORD

The work described in this report was supported by the National Aeronautics and Space Administration, Goddard Space Flight Center, under Contract NAS5-9978.

ABSTRACT

The hypersonic viscous layer at low Reynolds numbers with blowing has been analyzed in the stagnation region of a blunt body. By application of an integral method to the streamwise momentum, the normal momentum, and the energy equations, results are obtained for various values of the blowing rate and for various degrees of rarefaction of the flow. Significant effects of blowing on the character of the flow are observed.

TABLE OF CONTENTS

LIST OF SYMBOLS

a	Body nose radius
A	Skin-friction parameter, $(\partial U/\partial F)_b$
B	Heat-transfer parameter, $(\partial \Theta/\partial F)_b$
B_e	$= (\partial \Theta/\partial F)_e$
C	$= (\rho\mu)/(\rho_r\mu_r)$
C_H	Stanton number, $\left(k\frac{\partial T}{\partial y}\right)_b / [\rho_\infty U_\infty (H_\infty - H_b)]$
F	Transformed normal coordinate, eq. (7)
f	Dimensionless stream function, eq. (9)
G	Parameter for shock standoff distance, eq. (7)
H	Total enthalpy, $h + (u^2+v^2)/2$
h	Static enthalpy
j	Unity for axisymmetric flow and zero for planar flow
k	Thermal conductivity
K^2	Rarefaction parameter, $\epsilon(\rho_\infty U_\infty a/\mu_*)(T_*/T_o)$
M_i	Integrals involving U and Θ, Sec. 2.3
N	Blowing parameter, $(\rho_b v_b)/(\rho_\infty U_\infty)$
p	Pressure
P_r	Prandtl number
Q	$= P_r K^2 G$
r	Distance from the axis to the body surface
T	Temperature
T_*	Reference temperature, $(T_b + T_o)/2$
t_b	$= H_b/H_\infty$
U	Dimensionless streamwise velocity, $u/(U_\infty \cos\beta)$

u, v	Velocities in the physical coordinate (Fig. 2)
x, y	Physical coordinates (Fig. 2)
Z	$= r/a$
α	Defined in eq. (44b)
β	Angle (Fig. 2)
γ	Specific heat ratio
Δ	Shock standoff distance
ϵ	Density ratio across the shock
Θ	Enthalpy ratio, $(H - H_b)/(H_\infty - H_b)$
μ	Viscosity
ξ	Dimensionless streamwise distance, x/a
ρ	Density
ψ	Stream function

Subscripts

b	Body surface
e	Outer edge of the viscous shock layer
r	Reference condition
∞	Free-stream condition

1. INTRODUCTION

The purpose of the present report is to describe an integral method applied to the analysis of the effects of blowing on the viscous hypersonic shock layer (low Reynolds numbers) in the stagnation region of an Apollo-type entry body. This work represents the initial phase of a study undertaken in order to obtain a description of the viscous flow field in the entire forebody region.

A brief description of the physical characteristics of the hypersonic low Reynolds number flow as well as a short review of previous analyses will be given in this section, while the method of solution adopted in the present analysis and the discussion of results will be included in Sections 2 and 3, respectively.

One aspect of the low Reynolds number flow is that the thin boundary-layer approximation is no longer applicable in analyzing the flow around a blunt body at high altitudes.[1-4] For example, for an Apollo body, under typical re-entry conditions, the thin-boundary-layer assumption breaks down at altitudes greater than about 250,000 feet. At higher altitudes the influence of the transport properties is now spread across the shock layer and even the shock wave itself may not be thin compared to the shock standoff distance. Thus, a different type of flow will exist at these rarefied conditions. Delineation of the various flow regimes has been proposed[1] in terms of the degree of the rarefaction of the flow at high altitudes. Figure 1 shows these regimes in terms of a "rarefaction" parameter, K^2, introduced by Cheng.[2] For detailed discussion on these flow regimes, the reader is referred to References 1, 3 and 5.

Many analyses of the low Reynolds number flow are available, for example, References 1-3 and 6-16. All of these analyses used the Navier-Stokes equations and, except for Refs. 3 and 16, are confined to the stagnation region. In analyzing the stagnation region, solutions were obtained[1, 8] by assuming constant density in the shock layer. The results for heat transfer are in good agreement with those obtained by others (Refs.

2, 9). However, much higher shock standoff distance was obtained under constant-density assumption.[1,8] This assumption was later removed, and by assuming the shock layer to be very thin compared with the body radius, reasonable results were obtained (Refs. 6, 9).

As the mean free path becomes large, intermolecular collisions become less frequent and molecules arriving at the body surface are unable to come into equilibrium with the surface. As a result, velocity and temperature discontinuities may develop at the body surface. This is commonly called the "velocity slip" and the "temperature slip" at the wall. The effects of these wall-slip phenomena have been analyzed by Liu (Ref. 15). He found that these effects cause only a small change in the heat-transfer rate to the body as well as in the shock standoff distance.

One aspect of the rarefaction of the viscous flows at higher altitudes, i.e., low values of K^2, is that the shock wave is no longer thin or discontinuous. As a result, the usual Rankine-Hugoniot relationship is not quite applicable and should be modified in order to account for the transport effects immediately behind the now-thickened shock wave. This has been analyzed and the modified Rankine-Hugoniot relationships have been obtained by Probstein and Kemp[1] and by Cheng.[2]

The effects of mass injection in the stagnation region of a blunt body have been considered by Goldberg and Scala,[10] and Goldberg,[11] and Chen, Aerosty and Mobley.[12] Their results demonstrate increasing shock standoff distance and decreasing heat transfer with increasing injection rates. However, these changes are not as great at higher altitudes. Thus, for the rarefied-flow case, larger mass-injection rates are necessary to reduce the heat transfer coefficient by the same percentage as that for the boundary-layer flow case. No analyses are known to exist which treat the cases of very large mass-injection rates at locations away from the stagnation region.

The present formulation will now be briefly described. An axisymmetric flow over a blunt body with large blowing at the body surface is considered. The flow will be in the incipient-merged-layer at the viscous-

layer regimes. In these regimes, the Navier-Stokes equations may be used, and these equations are simplified by assuming a very thin shock layer compared with the body radius. In addition, the body is taken to be spherical so that the radius of curvature (a) is a constant in the present analysis. The streamwise velocity component at the body surface (u_b) is assumed to be zero, implying no-slip condition which is reasonable for a cold-wall[3] case, i. e., $T_b \to 0$. However, it can be included as a non-zero quantity without difficulty. For the present application of the cold-wall case, this is not necessary and zero-slip velocity is assumed at the wall.

The equations thus simplified are similar in form to the conventional boundary-layer equations with the important exceptions that the entire flow field is now viscous, instead of a very thin layer near the wall and that the normal pressure gradient may not be assumed negligible. The latter condition is associated with a non-negligible momentum change in the direction normal to the body surface.

The integral method was used in the present study because of the obvious advantages of the method over the exact analysis (which requires solution of the "two-point" boundary-value problem). These advantages are the ease of application and relatively small computation time. Results were obtained in the stagnation region for various values of the blowing rate (N), and of the "rarefaction parameter" (K^2). Significant effects of mass injection on heat transfer and shock standoff distance were observed. In what follows, the method of analysis for the present problem is presented in detail.

2. METHOD OF ANALYSIS

2.1 Differential Equations

The assumptions taken in the present analysis are:

1) thin shock layer,
2) hypersonic flow,
3) non-reacting gas,
4) constant Prandtl number, and
5) constant radius of curvature, i.e. a = const.

Applying these assumptions, the Navier-Stokes equations and other conservations equations become[3] for the viscous shock layer

Continuity:

$$\frac{\partial}{\partial x}(\rho u r^{j}) + \frac{\partial}{\partial y}(\rho v r^{j}) = 0 \qquad (1)$$

Streamwise Momentum:

$$\rho u \frac{\partial u}{\partial x} + \rho v \frac{\partial u}{\partial y} = -\frac{\partial p}{\partial x} + \frac{\partial}{\partial y}\left(\mu \frac{\partial u}{\partial y}\right) \qquad (2)$$

Normal Momentum:

$$\frac{\rho u^2}{a} = \frac{\partial p}{\partial y} \qquad (3)$$

Energy:

$$\rho u \frac{\partial H}{\partial x} + \rho v \frac{\partial H}{\partial y} = \frac{\partial}{\partial y}\left[\frac{\mu}{P_r}\frac{\partial H}{\partial y} + \frac{P_r - 1}{P_r}\mu\left(u\frac{\partial u}{\partial y} + v\frac{\partial v}{\partial y}\right)\right] \qquad (4)$$

State:

$$p = \rho R T \qquad (5)$$

where $H = h + (u^2+v^2)/2$, P_r = const. and other terms are shown in Figure 2.

The boundary conditions are

at $y=0$;

$$\begin{aligned} u &= 0 \\ v &= v_b(x) \\ p &= p_b(x) \\ H &= H_b(x) \end{aligned} \tag{6a}$$

at $y=\Delta$;

$$u = U_\infty \cos\beta - \frac{\mu_e}{\rho_\infty U_\infty \sin\beta}\left(\frac{\partial u}{\partial y}\right)_e$$

$$\rho_e v_e = -\rho_\infty U_\infty \sin\beta$$

$$p \cong \rho_\infty U_\infty^2 \sin^2\beta \tag{6b}$$

$$H = H_\infty - \frac{\mu_e}{Pr\,\rho_\infty U_\infty \sin\beta}\cdot\frac{\partial}{\partial y}\left(H + \frac{Pr-1}{2}u^2\right)_e$$

In the above boundary conditions the streamwise velocity component at the body surface u_b is assumed to be zero, implying no-slip condition which is reasonable for a cold-wall[3] case, i.e., $T_b \to 0$. However, it can be included as a non-zero quantity without difficulty. For the present application of the cold-wall case, this is not necessary and zero-slip velocity is assumed at the wall. It is also to be noted that the pressure distribution immediately behind the shock is Newtonian, in keeping with the thin shock-layer assumption.

Now we shall first transform the above differential equations from the (x, y) coordinate to the (ξ, F) coordinate system and then apply the integral method.

Introduce

$$\xi = \frac{x}{a}, \quad F = \frac{1}{G}\int_0^y \frac{\rho}{\rho_\infty}\cdot\frac{dy}{a} \tag{7}$$

where

$$G = \int_0^{\Delta(x)} \frac{\rho}{\rho_\infty}\frac{dy}{a}$$

In addition, introduce the stream function ψ such that

$$\frac{\partial \psi}{\partial x} = -(1+j)(\pi r)^j \rho v$$

$$\frac{\partial \psi}{\partial y} = (1+j)(\pi r)^j \rho u \tag{8}$$

Put

$$\psi = (1+j)\rho_\infty U_\infty r(\pi r)^j f \tag{9}$$

Then from eqs. (8) and (9) we obtain

$$u = \frac{U_\infty z}{G}\frac{\partial f}{\partial F}$$

where $z = r/a$. Putting $U = u/(U_\infty z)$, we get

$$U = \frac{1}{G}\frac{\partial f}{\partial F} \tag{10}$$

From eqs. (8) and (9) we also obtain

$$-\frac{\rho v}{\rho_\infty U_\infty} = (1+j)\frac{dz}{d\xi} f + z\frac{\partial f}{\partial \xi} + r\frac{\partial f}{\partial F}\left(\frac{\partial F}{\partial x}\right)_y \tag{11}$$

Applying the transformation eq. (7) to eq. (3) we get

$$\frac{\partial p}{\partial F} = \rho_\infty U_\infty^2 \frac{z^2}{G}\left(\frac{\partial f}{\partial F}\right)^2 \tag{12}$$

Also,

$$\frac{\partial p}{\partial x} = \frac{\partial p}{\partial \xi}\frac{d\xi}{dx} + \frac{\partial p}{\partial F}\left(\frac{\partial F}{\partial x}\right)_y = \frac{1}{a}\frac{\partial p}{\partial \xi} + \frac{\rho_\infty U_\infty^2 z^2}{G}\left(\frac{\partial f}{\partial F}\right)^2\left(\frac{\partial F}{\partial x}\right)_y \tag{13}$$

Equations (2), (3) and (4) become, after transformation,

ξ- Mom:

$$K^2 G\left[G\frac{\partial f}{\partial F}\cdot\frac{\partial}{\partial \xi}\left(\frac{z}{G}\frac{\partial f}{\partial F}\right) - (1+j)\frac{dz}{d\xi} f\frac{\partial^2 f}{\partial F^2} - z\frac{\partial f}{\partial \xi}\frac{\partial^2 f}{\partial F^2}\right]$$

$$= -\frac{K^2 G^3}{\rho U_\infty^2 z}\frac{\partial p}{\partial \xi} - K^2 a z G^2 \frac{\rho_\infty}{\rho}\left(\frac{\partial f}{\partial F}\right)^2\frac{\partial F}{\partial x} + \frac{\partial}{\partial F}\left(C\frac{\partial^2 f}{\partial F^2}\right) \tag{14}$$

F-Mom:

$$\frac{\partial p}{\partial F} = \rho_\infty U_\infty^2 \frac{z^2}{G}\left(\frac{\partial f}{\partial F}\right)^2 \tag{12}$$

Energy:

$$z\frac{dt_b}{d\xi}\frac{\partial f}{\partial F}(1-\theta) + z(1-t_b)\left(\frac{\partial f}{\partial F}\frac{\partial \theta}{\partial \xi} - \frac{\partial f}{\partial \xi}\frac{\partial \theta}{\partial F}\right) - (1+j)(1-t_b)\frac{dz}{d\xi} f\frac{\partial \theta}{\partial F}$$

$$= \frac{1-t_b}{P_r K^2 G}\cdot\frac{\partial}{\partial F}\left(C\frac{\partial \theta}{\partial F}\right) + \frac{P_r - 1}{P_r}\frac{2z^2}{K^2 G^3}\cdot\frac{\partial}{\partial F}\left(C\frac{\partial f}{\partial F}\cdot\frac{\partial^2 f}{\partial F^2}\right) \tag{15}$$

where

$$K^2 \equiv \epsilon R_e = \epsilon\frac{\rho_\infty U_\infty a}{\mu_r}, \qquad \theta = \frac{H - H_b}{H_\infty - H_b}$$

$$t_b = \frac{H_b}{H_\infty}, \qquad C \equiv \frac{\rho\mu}{\rho_r \mu_r} \tag{16}$$

and the subscript r denotes a reference condition. In the present analysis this condition will be taken[3] such that C = 1.

The difference between the boundary-layer approximation and the present analysis should be noted. In the boundary-layer analysis, the normal pressure gradient is negligibly small and is neglected; this in turn enables the second term on the right-hand side of eq. (13) to be dropped. In the present analysis this is not permissible and the term is retained, which contains the $(\partial F/\partial x)$ term. This term may be expressed in the (ξ, F) coordinate system as follows. We know that

$$\left(\frac{\partial}{\partial x}\right)_y = \frac{\partial}{\partial \xi}(\,)_F\cdot\frac{d\xi}{dx} + \frac{\partial}{\partial F}(\,)_\xi\cdot\left(\frac{\partial F}{\partial x}\right)_y$$

Therefore, $$\left(\frac{\partial y}{\partial x}\right)_y = 0 = \left(\frac{\partial y}{\partial \xi}\right)_F \frac{d\xi}{dx} + \left(\frac{\partial y}{\partial F}\right)_\xi \left(\frac{\partial F}{\partial x}\right)_y$$

or, $$\left(\frac{\partial F}{\partial x}\right)_y = -\frac{1}{a}\frac{(\partial y/\partial \xi)_F}{(\partial y/\partial F)_\xi} \tag{17}$$

From eq. (7) we have $(\partial y/\partial F)_\xi = \rho_\infty G a/\rho$

and $$y = G a \int_0^F \frac{\rho_\infty}{\rho} dF \tag{18}$$

Thus, eq. (17) becomes

$$\left(\frac{\partial F}{\partial x}\right)_y = -\frac{\rho}{\rho_\infty G a}\frac{\partial}{\partial \xi}\left(G\int_0^F \frac{\rho_\infty}{\rho} dF\right) \tag{19}$$

Equation (14) thus becomes, using eq. (19) and putting C = 1,

$$K^2 G\left[G\frac{\partial f}{\partial F}\frac{\partial}{\partial \xi}\left(\frac{z}{G}\frac{\partial f}{\partial F}\right) - (1+j)\frac{dz}{d\xi} f\frac{\partial^2 f}{\partial F^2} - z\frac{\partial f}{\partial \xi}\cdot\frac{\partial^2 f}{\partial F^2}\right]$$

$$= -\frac{K^2 G^3}{\rho U_\infty^2 z}\cdot\frac{\partial p}{\partial \xi} + K^2 G z\left(\frac{\partial f}{\partial F}\right)^2\frac{\partial}{\partial \xi}\left(G\int_0^F \frac{\rho_\infty}{\rho} dF\right) + \frac{\partial^3 f}{\partial F^3} \tag{20}$$

Now the term $\partial p/\partial \xi$ can be expressed in the (ξ, F) system as follows:
From eq. (12) we have

$$\frac{\partial p}{\partial F} = \rho_\infty U_\infty^2 \frac{z^2}{G}\left(\frac{\partial f}{\partial F}\right)^2 \tag{12}$$

Integrating from F = F to F = 1.0, we get

$$p(\xi, F) = p_e(\xi) - \rho_\infty U_\infty^2 \frac{z^2}{G}\int_F^1 \left(\frac{\partial f}{\partial F}\right)^2 dF \tag{21}$$

Therefore,

$$\frac{\partial p}{\partial \xi} = \frac{dp_e}{d\xi} - \rho_\infty U_\infty^2 \frac{\partial}{\partial \xi}\left(\frac{z^2}{G}\int_F^1 \left(\frac{\partial f}{\partial F}\right)^2 dF\right)_F \tag{22}$$

Substitution of eq. (22) in eq. (20) and use of $UG = (\partial f/\partial F)$ yields, after some rearrangements

$$K^2 G\left[G\frac{dz}{d\xi}U^2 + zGU\frac{\partial U}{\partial \xi} - (1+\beta)\frac{dz}{d\xi}f\frac{\partial U}{\partial F} - z\frac{\partial f}{\partial \xi}\frac{\partial U}{\partial F}\right]$$

$$= -\frac{K^2G^2}{\rho U_\infty^2 z}\frac{dp_e}{d\xi} + 2K^2G^3\frac{dz}{d\xi}\frac{\rho_\infty}{\rho}\int_F^1 U^2 dF + 2K^2G^2\frac{\rho_\infty}{\rho}\frac{\partial}{\partial \xi}\left(G\int_F^1 U^2 dF\right) \tag{23}$$

$$+ K^2G^2zU^2\frac{\partial}{\partial \xi}\left(G\int_0^F \frac{\rho_\infty}{\rho}dF\right) + \frac{\partial^2 U}{\partial F^2}$$

Before applying the integral method it is helpful to rearrange some terms in the streamwise momentum equation (23) and the energy equation (15) as follows:

Since

$$\frac{\partial f}{\partial \xi}\frac{\partial U}{\partial F} = \frac{\partial}{\partial F}\left(U\frac{\partial f}{\partial \xi}\right) - U\frac{\partial}{\partial \xi}(GU)$$

we get after some manipulations

$$GU\frac{\partial U}{\partial \xi} - \frac{\partial f}{\partial \xi}\frac{\partial U}{\partial F} = -\frac{\partial}{\partial \xi}\left[GU(1-U)\right] + \frac{\partial}{\partial F}\left[(1-U)\frac{\partial f}{\partial \xi}\right] \tag{24}$$

Also, using

$$\frac{\partial f}{\partial F}\frac{\partial \theta}{\partial \xi} = \frac{\partial}{\partial \xi}\left(\theta\frac{\partial f}{\partial F}\right) - \theta\frac{\partial}{\partial \xi}\left(\frac{\partial f}{\partial F}\right)$$

and

$$\frac{\partial f}{\partial \xi}\frac{\partial \theta}{\partial F} = \frac{\partial}{\partial F}\left(\theta\frac{\partial f}{\partial \xi}\right) - \theta\frac{\partial}{\partial \xi}\left(\frac{\partial f}{\partial F}\right)$$

We obtain

$$\frac{\partial f}{\partial F}\frac{\partial \theta}{\partial \xi} - \frac{\partial f}{\partial \xi}\frac{\partial \theta}{\partial F} = -\frac{\partial}{\partial \xi}\left[GU(1-\theta)\right] + \frac{\partial}{\partial F}\left[(1-\theta)\frac{\partial f}{\partial \xi}\right] \tag{25}$$

and

$$f\frac{\partial \theta}{\partial F} = -\frac{\partial}{\partial F}\left[f(1-\theta)\right] + GU(1-\theta) \tag{26}$$

Substitution of eq. (24) in eq. (23) and eqs. (25), (26) in eq. (15) then yields, respectively,

Streamwise Momentum:

$$K^2G\Big[G\frac{dz}{d\xi}\bar{U}^2-(1+j)\frac{dz}{d\xi}G\bar{U}(1-\bar{U})-z\frac{\partial}{\partial\xi}\{G\bar{U}(1-\bar{U})\}$$
$$+z\frac{\partial}{\partial F}\Big\{\frac{\partial f}{\partial\xi}(1-\bar{U})\Big\}+(1+j)\frac{dz}{d\xi}\frac{\partial}{\partial F}\{f(1-\bar{U})\}\Big]$$
$$=K^2G^2\frac{\rho_\infty}{\rho}\Big[-\frac{dp_e/d\xi}{\rho_\infty U_\infty^2 z}+2G\frac{dz}{d\xi}\int_F^1\bar{U}^2dF+z\frac{\partial}{\partial\xi}\Big(G\int_F^1\bar{U}^2dF\Big)\Big]$$
$$+zK^2G^2\bar{U}^2\frac{\partial}{\partial\xi}\Big(G\int_0^F\frac{\rho_\infty}{\rho}dF\Big)+\frac{\partial^2\bar{U}}{\partial F^2} \qquad (27)$$

Energy:

$$z(1-t_b)\frac{\partial}{\partial F}\Big[\frac{\partial f}{\partial\xi}(1-\Theta)\Big]+z\frac{dt_b}{d\xi}G\bar{U}(1-\Theta)-z(1-t_b)\frac{\partial}{\partial\xi}\Big[G\bar{U}(1-\Theta)\Big]$$
$$-(1+j)(1-t_b)\frac{dz}{d\xi}G\bar{U}(1-\Theta)+(1+j)(1-t_b)\frac{dz}{d\xi}\frac{\partial}{\partial F}\Big[f(1-\Theta)\Big] \qquad (28)$$
$$=\frac{1-t_b}{P_r K^2 G}\cdot\frac{\partial^2\Theta}{\partial F^2}+\frac{P_r-1}{P_r}\frac{2z^2}{K^2G}\frac{\partial}{\partial F}\Big(\bar{U}\frac{\partial\bar{U}}{\partial F}\Big)$$

2.2 The Boundary Conditions

The boundary conditions in the physical coordinate system, i.e., x-y plane, will now be expressed in the transformed (ξ, F) coordinate system. From eq. (11), specializing to the body surface, i.e., y = o (F = 0), we obtain

$$-\frac{\rho_b v_b}{\rho_\infty U_\infty}=(1+j)\frac{dz}{d\xi}f_b+z\frac{df_b}{d\xi} \qquad (29)$$

where $\bar{U}=0$ at F = 0 is applied.

Putting $N = (\rho_b v_b)/(\rho_\infty U_\infty)$ and integrating eq. (29), we get

$$f_b(\xi) = -\frac{\int_0^\xi z^j N(\xi)\,d\xi}{z^{1+j}} \tag{30}$$

For the special case, i.e., the stagnation point, $\xi \to 0$, and eq. (30) yields

$$f_b(0) = -\frac{N(0)}{1+j} \tag{31}$$

On the other hand, since the mass entering the shock layer from the free-stream is $r(\pi r)^j \rho_\infty U_\infty$, we have, by applying equation (9) at F = 1,

$$f_e = \frac{1}{1+j} = \text{constant} \tag{32}$$

Also, from eq. (6), we obtain, at F = 1

$$U_e = 1 - \frac{1}{K^2 G \sin\beta}\left(\frac{\partial U}{\partial F}\right)_e \tag{33}$$

and

$$\Theta_e = 1 - \frac{1}{P_r K^2 G \sin\beta}\left(\frac{\partial \Theta}{\partial F}\right)_e$$

It may be seen from Fig. 2 that $\sin\beta = \sqrt{1-z^2}$. Thus the Newtonian pressure distribution p_e becomes

$$p_e(\xi) = \rho_\infty U_\infty^2 (1 - z^2)$$

and

$$-\frac{dp_e/d\xi}{2\rho_\infty U_\infty^2 z} = \frac{dz}{d\xi} \tag{34}$$

From the relationship $GU = (\partial f/\partial F)$, we obtain, using eqs. (31) and (32)

$$G\int_0^1 U\,dF = f_e - f_b = \frac{1}{1+j} + \frac{\int_0^\xi z^j N\,d\xi}{z^{1+j}} \tag{35}$$

The physical shock-layer thickness (the shock standoff distance) may be obtained by applying eq. (18) at F = 1:

$$\frac{\Delta}{a} = G\int_0^1 \frac{\rho_\infty}{\rho}\,dF \tag{36}$$

Using the ideal gas relationship (eq. (5)), we have, for strong shock waves, i.e., M_∞ very large

$$\frac{\rho_\infty}{\rho} = \epsilon\left[t_b + (1-t_b)\,\Theta\right] \tag{37}$$

in the stagnation region, and eq. (36) becomes

$$\frac{\Delta}{a} = \epsilon G\left[t_b + (1-t_b)\int_0^1 \Theta\, dF\right] = \epsilon G M_3 \tag{38}$$

2.3 Integral Equations

The streamwise momentum equation (27) is now integrated from F = 0 to F = 1, i.e., from the body surface to the edge of the shock layer. Using eqs. (31), (32), (33) and (34), eq. (27) becomes

$$\begin{aligned}
&K^2 G \frac{dz}{d\xi}\left[\frac{1}{1+j} + \frac{\int_0^\xi z^j N\, d\xi}{z^{1+j}} - (2+j) M_1 G\right] - z K^2 G \frac{d}{d\xi}(G M_1) + N K^2 G \\
&= 2K^2 G^2 \frac{dz}{d\xi}\int_0^1 \frac{\rho_\infty}{\rho}\left(1 + G\int_F^1 U^2 dF\right) dF + z K^2 G^3 \int_0^1 \frac{\rho_\infty}{\rho}\frac{\partial}{\partial\xi}\left(\int_F^1 U^2 dF\right) dF \\
&+ z K^2 G^2 \frac{dG}{d\xi}\left[\int_0^1 \frac{\rho_\infty}{\rho}\cdot\int_F^1 U^2 dF\cdot dF + \int_0^1 U^2\cdot\int_0^F \frac{\rho_\infty}{\rho} dF\cdot dF\right] \\
&+ z K^2 G^3 \frac{d}{d\xi}\left[\int_0^1 U^2\cdot\int_0^F \frac{\rho_\infty}{\rho} dF\cdot dF\right] - A - z K^2 G^3 \int_0^1 \left(\frac{\partial U}{\partial \xi}\right)^2 \cdot \int_0^F \frac{\rho_\infty}{\rho} dF\cdot dF
\end{aligned} \tag{39}$$

where $M_1 = \int_0^1 U(1-U)\, dF$.

Integration of the energy equation (25) from F = 0 to F = 1 yields, after some rearrangements

$$\frac{d}{d\xi}\left[G(1-t_b) z^{1+j} M_5\right] = z^j (1-t_b)\left[N + \frac{B}{P_r K^2 G} - \frac{P_r - 1}{P_r}\cdot\frac{2 z^2 U_e A_e}{K^2 G (1-t_b)}\right] \tag{40}$$

where

$$B = \left(\frac{\partial \Theta}{\partial F}\right)_{F=0} \quad , \qquad A_e = \left(\frac{\partial U}{\partial F}\right)_{F=1}$$

and

$$M_5 = \int_0^1 U\,(1-\Theta)\,dF$$

Thus, we have derived two integral equations which involve the integrals of U and Θ with respect to F for various values of the rarefaction parameter (K^2), mass-injection rate (N), and the Prandtl Number (Pr). Before proceeding downstream, the present formulation will be applied to the stagnation region. This serves a two fold purpose; first, it serves as a check against a previous analysis of Cheng[2] for a zero mass-injection case in the stagnation region; secondly, it furnishes the initial conditions for equations (39) and (40).

Specializing to the stagnation region, i.e., $\xi \to 0$, and $\frac{dz}{d\xi} \to 1$, eqs. (39) and (40) reduce to, after some manipulations,

$$K^2 G\left[(2+j)M_1 G + 2\epsilon M_{3a} G - \frac{1+(2+j)N}{1+j}\right] = A \qquad (41)$$

and

$$(1+j)\,G\,M_5 = N + \frac{B}{P_r K^2 G} \qquad (42)$$

where a new term M_{3a} is introduced by using eq. (37):

$$M_{3a} = \int_0^1 \left[t_b + (1-t_b)\Theta\right]\cdot\left[1 + G\int_F^1 U^2 dF\right]\cdot dF$$

2.4 Velocity and Energy Profiles

In order to solve the eqs. (41) and (42), we now introduce profiles for the streamwise velocity U and the total-enthalpy Θ in terms of the characteristic parameters. Since there are two equations, two parameters will be introduced, i.e., G and B. This implies that both U and Θ profiles are one-parameter families, i.e., $U = U(F; G)$ and $\Theta = \Theta(F; B, G)$. It will be seen from the results that these simple forms yield reasonable results even in cases of very large mass-injection rates N and a wide range of the rarefaction parameter K^2. The reason may be due to the use of reasonable boundary conditions as well as the applicability of the integral method with good accuracy to the favorable pressure gradient cases.

Streamwise Velocity Profiles:

Put $$U = a_1 F + a_2 F^2 + a_3 F^3 \tag{43}$$

where the coefficients a_1, a_2, a_3 are to be determined as follows.

The boundary conditions are:

From eq. (33), we get, for the stagnation region

$$U_e = 1 - \frac{1}{K^2 G}\left(\frac{\partial U}{\partial F}\right)_e \tag{44a}$$

From eq. (35), specializing to the stagnation point

$$\int_0^1 U\, dF = \frac{1}{G}\left(\frac{1+N}{1+j}\right) = \alpha \tag{44b}$$

Applying eq. (27) to the wall ($F = 0$) at the stagnation point,

$$\left(\frac{\partial^2 U}{\partial F^2}\right)_b + 2\epsilon_b K^2 G^2 \left(1 + G\int_0^1 U^2 dF\right) = K^2 G N \left(\frac{\partial U}{\partial F}\right)_b \tag{44c}$$

Substitution of eq. (43) in eqs. (44a) and (44b) yields

$$U = \frac{1}{E_1}\left(E_2 F^2 - E_3 F^3\right) + \frac{A}{E_1}\left(E_1 F - E_4 F^2 + E_5 F^3\right) \qquad (45)$$

where

$$E_1 = 1 + \frac{6}{K^2 G}$$

$$E_2 = 12\alpha\left(1 + \frac{3}{K^2 G}\right) - 3$$

$$E_3 = 12\alpha\left(1 + \frac{2}{K^2 G}\right) - 4$$

$$E_4 = 3\left(1 + \frac{5}{K^2 G}\right)$$

$$E_5 = 2\left(1 + \frac{4}{K^2 G}\right)$$

The skin-friction parameter $A = (\partial U/\partial F)_b$ may be determined from eq. (44c) by applying eq. (45),

$$A = \frac{-E_6 \pm \sqrt{E_6^2 - 4E_7 E_8}}{2E_7}$$

It is noted that two roots of A are involved in the present analysis, since we take into account the normal momentum term (the $\int_0^1 U^2 dF$ term in eq. (44c)). By comparing the above equation with the case where this centrifugal effect is neglected, we conclude that the lower root is the correct value. Thus we have

$$A = \frac{-E_6 - \sqrt{E_6^2 - 4E_7 E_8}}{2E_7} \qquad (46)$$

where

$$E_6 = E_9 - \frac{2E_1 E_4 + K^2 G N E_1^2}{2\epsilon t_b K^2 G^3}$$

$$E_7 = E_1\left(\frac{E_1}{3} - \frac{E_4}{2} + \frac{2}{5}E_5\right) + E_4\left(\frac{E_4}{5} - \frac{E_5}{3}\right) + \frac{E_5^2}{7}$$

$$E_8 = E_{10} + \frac{E_1^2}{G} + \frac{E_1 E_2}{\epsilon t_b K^2 G^3}$$

$$E_9 = E_1\left(\frac{E_2}{2} - \frac{2}{5}E_3\right) + E_2\left(\frac{E_5}{6} - \frac{E_4}{5}\right)$$

$$E_{10} = \frac{E_2^2}{5} - \frac{E_2 E_3}{3} + \frac{E_3^2}{7}$$

It is also to be noted that for given values of K^2, ϵ, N and t_b, A can be obtained from eq. (46) as a function of G, a characteristic parameter to be determined from the simultaneous solution of the integral equations (41) and (42).

Total-Enthalpy Profiles:

Put
$$\Theta = b_1 F + b_2 F^2 + b_3 F^3 + b_4 F^4 \qquad (47)$$

where the coefficients b_1, b_2, etc., are to be determined as follows. The boundary conditions are as follows:

From eq. (33)

$$\Theta_e = 1 - \frac{1}{P_r K^2 G}\left(\frac{\partial\Theta}{\partial F}\right)_e \qquad (48a)$$

Applying eq. (15) to the wall ($F = 0$) in the stagnation region, we have, using eq. (31) for f_b;

$$\left(\frac{\partial^2\Theta}{\partial F^2}\right)_b = P_r K^2 G N \left(\frac{\partial\Theta}{\partial F}\right)_b \qquad (48b)$$

Equation (15), when specialized to $F = 1$ in the stagnation region, becomes, using eq. (31) for f_e:

$$\left(\frac{\partial\Theta}{\partial F}\right)_e + \frac{1}{P_r K^2 G}\left(\frac{\partial^2\Theta}{\partial F^2}\right)_e = 0 \qquad (48c)$$

Solving eqs. (47), (48a), (48b) and (48c) simultaneously, we obtain

$$\Theta = \frac{N_{11}F^3 - N_{12}F^4}{N_{10}} + \frac{B}{N_{10}}\left(N_{10}F + \frac{QNN_{10}}{2}F^2 - N_8 F^3 + N_9 F^4\right) \qquad (49)$$

where $Q = R_t K^2 G$

$$N_8 = 3\left(1+\frac{2}{Q}\right)^2 + QN\left(1+\frac{5}{Q}+\frac{8}{Q^2}\right)$$

$$N_9 = 2\left(1+\frac{3}{Q}+\frac{3}{Q^2}\right) + \frac{QN}{2}\left(1+\frac{4}{Q}+\frac{6}{Q^2}\right)$$

$$N_{10} = 1+\frac{6}{Q}+\frac{12}{Q^2}$$

$$N_{11} = 4\left(1+\frac{3}{Q}\right)$$

$$N_{12} = 3\left(1+\frac{2}{Q}\right)$$

In equation (49), the parameter B is the unknown quantity to be determined along with G from the simultaneous solution of the integral equations (41) and (42).

Based on the profiles from eqs. (45), (49) and (37), it is now possible to calculate the terms included in the eqs. (41) and (42). Specifically, the "momentum-defect thickness" M_1 is recast in terms of M_2, using eq. (44b)

$$M_1 = \int_0^1 U(1-U)\,dF = \int_0^1 U\,dF - \int_0^1 U^2\,dF = \alpha - M_2 \qquad (50a)$$

and

$$M_2 = \int_0^1 U^2\,dF = N_5 + A N_6 + A^2 N_7 \qquad (50b)$$

where $N_1 = \epsilon t_b K^2 G^2$, $N_2 = 4\alpha G + \frac{4}{3}N_1$, $N_3 = \frac{K^2 G N}{2}$, $N_4 = 2 + \frac{4}{3}N_3$

$$N_5 = \frac{240(1+N)^2 + 20G N_1(1+j)(1+N) + (1+j)G^2 N_1^2}{105(1+j)^2 G^2}$$

$$-N_6 = \frac{13(1+j)GN_1 + 144(1+N) + 40N_3(1+N) + 4(1+j)N_1 N_3 G}{210(1+j)G}$$

$$N_7 = \frac{22 + N_3(13 + 2N_3)}{210}$$

From eqs. (45) and (49) we get

$$M_5 = \int_0^1 U(1-\theta)\,dF = N_{13} + AN_{14} - B(N_{15} + AN_{16}) \qquad (50c)$$

where

$$N_{13} = \frac{3N_6}{N_{10}}\left(\frac{1}{14} + \frac{5}{7Q} + \frac{4}{Q^2}\right) - \frac{N_1}{42N_{10}}\left(1 + \frac{6}{Q}\right)$$

$$N_{14} = \frac{1}{14N_{10}}\left[\frac{13}{10} + \frac{37}{5Q} + \frac{N_3}{3}\left(1 + \frac{6}{Q}\right)\right]$$

$$N_{15} = \frac{3N_6}{35N_{10}}\left(1 + \frac{11}{Q} + \frac{67}{Q^2}\right) - \frac{N_1}{35N_{10}}\left(\frac{1}{4} + \frac{3}{2Q} - \frac{2}{Q^2}\right)$$

$$- \frac{QNN_1}{70N_{10}}\left(\frac{1}{18} + \frac{1}{3Q} - \frac{1}{Q^2}\right) + \frac{\alpha QN}{7N_{10}}\left(\frac{1}{12} + \frac{1}{Q} + \frac{13}{2Q^2}\right)$$

$$N_{16} = \frac{1}{14N_{10}}\left(\frac{1}{3} + \frac{9}{5Q} - \frac{19}{5Q^2}\right) + \frac{N_3}{35N_{10}}\left(\frac{1}{4} + \frac{3}{2Q} - \frac{2}{Q^2}\right)$$

$$+ \frac{QN}{28N_{10}}\left(\frac{1}{15} + \frac{1}{3Q} - \frac{9}{5Q^2}\right) + \frac{QNN_3}{70N_{10}}\left(\frac{1}{18} + \frac{1}{3Q} - \frac{1}{Q^2}\right)$$

From eq. (49), we also obtain at F = 1

$$\theta_e = \frac{N_{11} - N_{12}}{N_{10}} + \frac{B}{N_{10}}\left(N_{10} + \frac{QNN_{10}}{2} - N_8 + N_9\right) \qquad (50d)$$

Therefore, substituting eq. (50c) for M_5, eq. (50d) for θ_e, we can express B in terms of G and other parameters so that

$$B = \frac{N_{18}}{N_{17}} \qquad (51)$$

where

$$N_{17} = (1+j)QGN_{10}(N_{15} + AN_{16}) + 1 + \frac{12}{Q} + \frac{6}{Q^2} + N\left(1 - \frac{1}{Q}\right)$$

$$N_{18} = (1+j)QGN_{10}(N_{13} + AN_{14}) + 1 + \frac{18}{Q} - QN_{10}(1+N)$$

We shall now rearrange the momentum-integral eq. (41) in a more convenient form. Substitution of eqs. (37), (45) and (49) in the definition of M_{3a} yields

$$M_{3a} = M_3 (1+GM_2) - \frac{G}{E_1^2}(E_{11} + AE_{12} + A^2E_{13}) - \frac{(1-t_b)G}{E_1^2 N_{10}}\left[E_{61} + AE_{62} + A^2E_{63} + B(E_{64} + AE_{65} + A^2E_{66})\right] \tag{52}$$

and

$$M_3 = \int_0^1 [t_b + (1-t_b)\Theta]\,dF = t_b + \frac{1-t_b}{N_{10}}(E_{67} + BE_{68}) \tag{53}$$

where the E_i's are included in the Appendix.

Summarizing, then we have derived two integral equations involving two parameters G and B, which will be obtained by simultaneous solution of these equations, i.e., using eq. (46) in eq. (41).

Momentum:

$$2K^2GE_7\left[(2+j)M_1G + 2\epsilon M_{3a}G - \frac{1+N(2+j)}{1+j}\right] = -E_6 - \sqrt{E_6^2 - 4E_7E_8} \tag{54}$$

Energy:

$$B = \frac{N_{18}}{N_{17}} \tag{51}$$

3. RESULTS AND DISCUSSION

Eqs. (51) and (54) were solved for the unknown parameters G and B for given values of the rarefaction parameter (K^2), mass-injection rate (N), density ratio across the shock (ϵ), and the wall-temperature (t_b). Because of the complicated way in which G and B are related in the eqs. (51) and (54), the following method of solution was applied.

1. For given input values of K^2, ϵ and t_b, the equations are functions of G, B, and N. Consider the $N = 0$ case, i.e., no mass injection. Start from a very low value of G, example, $G = 0.05$.

2. For the assumed value of G, compute B from eq. (51).

3. Substitute both G and B in eq. (54) and see it the left-hand side and the right-hand side of the equation are the same.

4. If not, assume a larger value of G, and repeat steps 2 and 3, until eq. (54) is satisfied.

5. Now put a new value of N in the eqs. (51) and (54).

6. Start from the value of G obtained from step 4, i.e., G for the lower mass-injection rate. Repeat steps 2, 3, and 4.

It is noted that step 6 is reasonable, since for greater mass-injection rates the value of G will be greater. This is due to the physical reasoning that greater mass injection will bring about a thicker shock layer, whose thickness is proportional to the value of G.

Results were obtained for $0.01 \leq K^2 \leq 500$, $0 \leq N \leq 1.0$ (100% mass-injection rate), $\epsilon = 0.1$, $Pr = 0.75$, $t_b = 0.05$ (very cold wall), on an IBM 360 digital computer. The computation time for a typical case was about 0.006 min. The results are shown in Figures 3-9.

Figure 3 gives the values of G obtained for various values of blowing rates and rarefaction parameter in the stagnation region. The term G is a measure of the shock standoff distance in the transformed plane. Previous analysis[2] for the no-blowing case gives, in the present notation, $G = (2/K^2) \Big/ \left[\sqrt{1 + \frac{4}{K^2}} - 1 \right]$. This result is also included in Fig. 3, and comparison with the present analysis is seen to be reasonable.

The heat-transfer rate is a convenient parameter with which comparison can be made between the results of the present formulation and those of Cheng[2] for the limiting condition of no mass injection. The heat-transfer rate at various altitudes, i.e., various values of K^2 (where $K^2 = \epsilon \left(\frac{\rho_\infty U_\infty L}{\mu_*} \right) \left(\frac{T_*}{T_0} \right)$, has been calculated for several values of the mass-injection parameter, $N \left(= \frac{\rho_b V_b}{\rho_\infty U_\infty} \right)$, for N ranging from 0 to 1.0 and the results are given in Figure 4. The heat-transfer rate is expressed in terms of the Stanton Number, i.e., $C_H = \left(k \frac{\partial T}{\partial y} \right)_b \Big/ \left[\rho_\infty U_\infty (H_\infty - H_b) \right]$. It may be seen from Figure 4 that, as the mass-injection rate increases for a given value of K^2, the heat-transfer rate to the body decreases, a result consistent with other analyses performed for boundary-layer flows[17, 18] and for viscous flows.[12] It is interesting to note that at lower altitudes, i.e., K^2 large, the effect of mass injection on the reduction in the heat-transfer rate is greater, while at higher altitudes this effect is smaller. In other words, a mass-injection ratio of 50 per cent, i.e., $N = 0.5$, brings about a sharp decrease in the heat-transfer rate at large values of K^2, while causing only a small reduction at small values of K^2. Thus a greater mass-injection rate is required at higher altitudes than is required at lower altitudes in order to reduce the heat-transfer coefficient by the same percentage. This result may stem from the relative ineffectiveness of the low-density fluid existing at the higher altitudes to respond to mass injection at the body surface. This is more clearly seen by taking the free-molecular limit, i.e., $K^2 \longrightarrow 0$. Since there is no intermolecular collision in this regime, the effect of mass injection on heat transfer from a cold wall is zero for a unit thermal accommodation coefficient. The results shown in Figure 4 for various mass-injection rates confirm this trend; The curves all converging to the result corresponding to the zero mass-injection case, as the free-molecular limit is approached ($K^2 \longrightarrow 0$). Also included in Figure 4 is

a result obtained by Cheng[2] for the N = 0 case. The agreement of the present result with that of Cheng for N = 0 is good. The minor discrepancy that does exist is due to the different values of the Prandtl Number, and in part, the result of differences in the method of solution. It should be noted that as K^2 becomes very small, C_H approaches unity asymptotically, a free-molecular result for unit thermal accommodation coefficient. Thus, although the present analysis is restricted to cases where $K^2 \gg 1.0$ (due to the thin shock-layer assumption), the extrapolation to more rarefied regimes yields quantitatively reasonable results.

Another interesting result is the influence of K^2 and mass-injection on the thickness of the viscous shock-layer, i.e., the shock standoff distance. Figure 5 shows the thickness Δ/a at different altitudes (K^2) for a special case of zero mass injection. For this case, a previous analysis of Cheng[2] is available, and comparison shows good agreement. Also shown are the changes in $\frac{\Delta}{a}$ due to mass injection for various values of K^2. It is seen that the thickness increases with increased mass injection rates, a result which is consistent with the results obtained in References 12 and 19. This is a physically reasonable result since the injected fluid adds mass to the flow which does not have a streamwise-momentum component and thus must be accelerated by the viscous-layer fluid. Thus, the streamwise-velocity component decreases at a given distance from the body surface, signifying a reduction in the local mass flux in the streamwise direction. Hence, in order to satisfy the requirement of the mass conservation, the velocity component in the direction normal to the body surface must increase with increased blowing. The net result is that the effect of mass injection is now felt further away from the body, thus increasing the region of the viscous influence, i.e., the viscous shock-layer thickness. There are analyses[11, 12] treating mass injection in the stagnation region of a viscous layer. Direct quantitative comparison with the present results is not easy to make, because of the differences in the formulation and the assumptions involved. It is noted, however, that the present results in terms of heat transfer and the shock standoff distances are in qualitative agreement with the results obtained in previous analyses.

The modified Rankine-Hugoniot relationship indicates that the total-enthalpy ratio of the flow decreases across the shock wave due to the transport effects. In addition, the velocity component tangential to the shock wave ($\bar{U}$) decreases across the shock wave. These results are shown in Figures 6 and 7 for N = 0 case. Agreement with the results in previous analysis[2] is excellent. The effects of mass injection on Θ_e and $\bar{U}_e$ at various altitudes are shown in Figures 8 and 9, and the results demonstrate the pronounced effects of blowing on these values.

4. CONCLUSIONS

The effects of blowing on the rarefied hypersonic shock layer in the stagnation region of a blunt body have been analyzed by application of an integral method. The results show significant effects of blowing on the flow characteristics, especially in the reduction in heat transfer and the increase in the shock standoff distances. However, these influences are observed to diminish as the Reynolds number decreases, i.e., increasing rarefaction. Where appropriate, comparison has been made with other analyses, and the present results are in reasonable agreement, demonstrating the applicability of an integral method to the analysis of the effects of blowing on the hypersonic viscous shock layer at low Reynolds numbers.

REFERENCES

1. Probstein, R. F. and Kemp, N. H., "Viscous Aerodynamic Characteristics in Hypersonic Rarefied Gas Flow," J. Aero. Sci., 27, #3, pp. 174-192, 218 (1960).

2. Cheng, H. K., "Hypersonic Shock-Layer Theory of the Stagnation Region at Low Reynolds Number," Proc. 1961 Heat Transfer and Fluid Mechanics Institute, Univ. of So. California, Stanford U. Press, pp. 161-175 (1961).

3. Cheng, H. K., "The Blunt-Body Problem in Hypersonic Flow at Low Reynolds Number," Cornell Aero. Lab. Rept. AF-1285-A-10 (June 1963).

4. Scala, S. M., "Hypersonic Viscous Shock Layer," ARS J. 29, pp. 520-522 (1959).

5. Hayes, W. D., and Probstein, R. F., Hypersonic Flow Theory, Academic Press (1959).

6. Ho, H. T., and Probstein, R. F., "The Compressible Viscous Layer in Rarefied Hypersonic Flow," Proc. Second Rarefied Gas Dynamics Symp., Academic Press, pp. 525-552 (1960).

7. Chung, P. M., "Hypersonic Viscous Shock Layer of Nonequilibrium Dissociating Gas," NASA TR R-109 (1961).

8. Oguchi, H., "Blunt Body Viscous Layer with and without Magnetic Field," Phys. Fluids, 3, #4, pp. 567-580 (1960).

9. Levinsky, E. S., and Yoshihara, H., "Rarefied Hypersonic Flow Over a Sphere," Progress in Astronautics and Rocketry, Vol. 7, Ed. F. Riddell, Academic Press, pp. 81-106 (1962).

10. Goldberg, L and Scala, S. M., "Mass Transfer in the Hypersonic Low Reynolds Number Viscous Layer," I. A. S. Paper No. 62-80 (1962).

11. Goldberg, L., "The Structure of the Viscous Hypersonic Shock Layer," G. E. Rept. R65SD50 (Dec. 1965).

12. Chen, S. Y., Aroesty, J. and Mobley, R., "The Hypersonic Viscous Shock Layer with Mass Transfer," Int. J. Heat Mass Transfer, 10, pp. 1143-1158 (1967).

13. Tong, H., "Effects of Dissociation Energy and Vibrational Relaxation on Heat Transfer," AIAA J. 4, #1, pp. 14-18 (1966).

14. Inger, G. R., "Nonequilibrium Hypersonic Stagnation Flow with Arbitrary Surface Catalycity Including Low Reynolds Number Effects," Int. J. Heat Mass Transfer 9, #8, pp. 755-772 (1966).

15. Liu, J. C. T., "The Effect of Wall Temperature on the Low Reynolds Number Hypersonic Stagnation Region Shock Layer," Int. J. Heat Mass Transfer, 10, pp. 83-95 (1967).

16. Bush, W. B., "On the Viscous Hypersonic Blunt-Body Problem," J. Fl. Mech. 20, Pt. 3, pp. 353-367 (1964).

17. Libby, P. A., "The Homogeneous Boundary Layer at an Axisymmetric Stagnation Point with Large Rates of Injection," J. Aerospace Sci., 29, pp. 48-60 (1962).

18. Kang, S. W., Rae, W. J. and Dunn, M. G., "Effects of Mass Injection on Compressible, Three-Dimensional, Laminar Boundary Layers,"AIAA J., 5, #10, pp. 1738-1745 (1967).

19. Howe, J. T. and Viegas, J. R., "Solutions of the Ionized Radiating Shock Layer, Including Reabsorption and Foreign Species Effects, and Stagnation Region Heat Transfer," NASA TR R-159 (1963).

Appendix A

DEFINITION OF FLOW INTEGRALS

The definitions for M_{3a} and M_3 are given in the text as eq. (52) and eq. (53), respectively. They are:

$$M_{3a} = M_3 (1 + M_2 G) - \frac{G}{E_1^2} (E_{11} + A E_{12} + A^2 E_{13}) - \frac{(1-t_b) G}{E_1^2 N_{10}} \left[E_{61} + A E_{62} + A^2 E_{63} + B (E_{64} + A E_{65} + A^2 E_{66}) \right] \quad (52)$$

and

$$M_3 = \int_0^1 [t_b + (1-t_b)\Theta] dF = t_b + \frac{1-t_b}{N_{10}} (E_{67} + B E_{68}) \quad (53)$$

where

$$E_{67} = \frac{1}{5} \left(2 + \frac{9}{Q} \right)$$

$$E_{68} = \frac{3}{20} \left(1 + \frac{8}{Q} + \frac{28}{Q^2} \right) + \frac{QN}{60} \left(1 + \frac{9}{Q} + \frac{36}{Q^2} \right)$$

$$E_{11} = \frac{E_2^2}{30} - \frac{E_2 E_3}{21} + \frac{E_3^2}{56}$$

$$E_{12} = \frac{E_1 E_2}{10} - \frac{E_1 E_3 + E_2 E_4}{15} + \frac{E_2 E_5 + E_3 E_4}{21} - \frac{E_3 E_5}{28}$$

$$E_{13} = \frac{E_1^2}{12} - \frac{E_1 E_4}{10} + \frac{E_4^2 + 2 E_1 E_5}{30} - \frac{E_4 E_5}{21} + \frac{E_5^2}{56}$$

$$E_{14} = \frac{E_2^2 N_{11}}{5}$$

$$E_{15} = - E_2 \left(\frac{N_{12} E_2}{5} + \frac{N_{11} E_3}{3} \right)$$

$$E_{16} = E_3 \left(\frac{N_{12} E_2}{3} + \frac{N_{11} E_3}{7} \right)$$

$$E_{17} = -\frac{E_3^2 N_{12}}{7}$$

$$E_{18} = \frac{E_1 E_2 N_{11}}{2}$$

$$E_{19} = -\left[\frac{2}{5}(E_1 E_3 + E_2 E_4) N_{11} + \frac{N_{12}}{2} E_1 E_2\right]$$

$$E_{20} = \frac{N_{11}}{3}(E_2 E_5 + E_3 E_4) + \frac{2}{5}(E_1 E_3 + E_2 E_4) N_{12}$$

$$E_{21} = -\left[\frac{2}{7} E_3 E_5 N_{11} + \frac{N_{12}}{3}(E_2 E_5 + E_3 E_4)\right]$$

$$E_{22} = \frac{2}{7} N_{12} E_3 E_5$$

$$E_{23} = \frac{N_{11} E_1^2}{3}$$

$$E_{24} = -E_1\left(\frac{E_4 N_{11}}{2} + \frac{E_1 N_{12}}{3}\right)$$

$$E_{25} = \frac{N_{11}}{5}(2E_1 E_5 + E_4^2) + \frac{E_1 E_4 N_{12}}{2}$$

$$E_{26} = -\left[\frac{E_4 E_5 N_{11}}{3} + \frac{N_{12}}{5}(2E_1 E_5 + E_4^2)\right]$$

$$E_{27} = E_5\left(\frac{E_4 N_{12}}{3} + \frac{E_5 N_{11}}{7}\right)$$

$$E_{28} = -\frac{E_5^2 N_{12}}{7}$$

$$E_{29} = \frac{E_2^2 N_{10}}{5}$$

$$E_{30} = \frac{Q N N_{10} E_2^2}{10} - \frac{N_{10} E_2 E_3}{3}$$

$$E_{31} = \frac{N_{10} E_3^2}{7} - \frac{Q N N_{10} E_2 E_3}{6} - \frac{N_8 E_2^2}{5}$$

$$E_{32} = \frac{Q N N_{10} E_3^2}{14} + \frac{N_8 E_2 E_3}{3} + \frac{N_9 E_2^2}{5}$$

$$E_{33} = -\frac{N_8 E_3^2}{7} - \frac{N_9 E_2 E_3}{3}$$

$$E_{34} = \frac{N_9 E_3^2}{7}$$

$$E_{36} = \frac{N_{10} E_1 E_2}{2}$$

$$E_{37} = \frac{QNN_{10} E_1 E_2}{4} - \frac{2N_{10}}{5}(E_1 E_3 + E_2 E_4)$$

$$E_{38} = \frac{N_{10}}{3}(E_2 E_5 + E_3 E_4) - \frac{QNN_{10}}{5}(E_1 E_3 + E_2 E_4) - \frac{N_8 E_1 E_2}{2}$$

$$E_{39} = -\frac{2N_{10} E_3 E_5}{7} + \frac{QNN_{10}}{6}(E_2 E_5 + E_3 E_4) + \frac{2N_8}{5}(E_1 E_3 + E_2 E_4) + \frac{N_9 E_1 E_2}{2}$$

$$E_{40} = -\frac{QNN_{10} E_3 E_5}{7} - \frac{N_8}{3}(E_2 E_5 + E_3 E_4) - \frac{2N_9}{5}(E_1 E_3 + E_2 E_4)$$

$$E_{41} = \frac{2N_8 E_3 E_5}{7} + \frac{N_9}{3}(E_2 E_5 + E_3 E_4)$$

$$E_{42} = -\frac{2N_9 E_3 E_5}{7}$$

$$E_{44} = \frac{N_{10} E_1^2}{3}$$

$$E_{45} = -\frac{N_{10} E_1 E_4}{2} + \frac{QNN_{10} E_1^2}{6}$$

$$E_{46} = \frac{N_{10}}{5}(E_4^2 + 2E_1 E_5) - \frac{QNN_{10} E_1 E_4}{4} - \frac{N_8 E_1^2}{3}$$

$$E_{47} = -\frac{N_{10} E_4 E_5}{3} + \frac{QNN_{10}}{10}(E_4^2 + 2E_1 E_5) + \frac{N_8 E_1 E_4}{2} + \frac{N_9 E_1^2}{3}$$

$$E_{48} = \frac{N_{10} E_5^2}{7} - \frac{QNN_{10} E_4 E_5}{6} - \frac{N_8}{5}(E_4^2 + 2E_1 E_5) - \frac{N_9 E_1 E_4}{2}$$

$$E_{49} = \frac{QNN_{10} E_5^2}{14} + \frac{N_8 E_4 E_5}{3} + \frac{N_9}{5}(E_4^2 + 2E_1 E_5)$$

$$E_{50} = -\frac{N_8 E_5^2}{7} - \frac{N_9 E_4 E_5}{3}$$

$$E_{51} = \frac{N_9 E_5^2}{7}$$

$$E_{61} = \frac{E_{14}}{9} + \frac{E_{15}}{10} + \frac{E_{16}}{11} + \frac{E_{17}}{12}$$

$$E_{62} = \frac{E_{18}}{8} + \frac{E_{19}}{9} + \frac{E_{20}}{10} + \frac{E_{21}}{11} + \frac{E_{22}}{12}$$

$$E_{63} = \frac{E_{23}}{7} + \frac{E_{24}}{8} + \frac{E_{25}}{9} + \frac{E_{26}}{10} + \frac{E_{27}}{11} + \frac{E_{28}}{12}$$

$$E_{64} = \frac{E_{29}}{7} + \frac{E_{30}}{8} + \frac{E_{31}}{9} + \frac{E_{32}}{10} + \frac{E_{33}}{11} + \frac{E_{34}}{12}$$

$$E_{65} = \frac{E_{36}}{6} + \frac{E_{37}}{7} + \frac{E_{38}}{8} + \frac{E_{39}}{9} + \frac{E_{40}}{10} + \frac{E_{41}}{11} + \frac{E_{42}}{12}$$

$$E_{66} = \frac{E_{44}}{5} + \frac{E_{45}}{6} + \frac{E_{46}}{7} + \frac{E_{47}}{8} + \frac{E_{48}}{9} + \frac{E_{49}}{10} + \frac{E_{50}}{11} + \frac{E_{51}}{12}$$

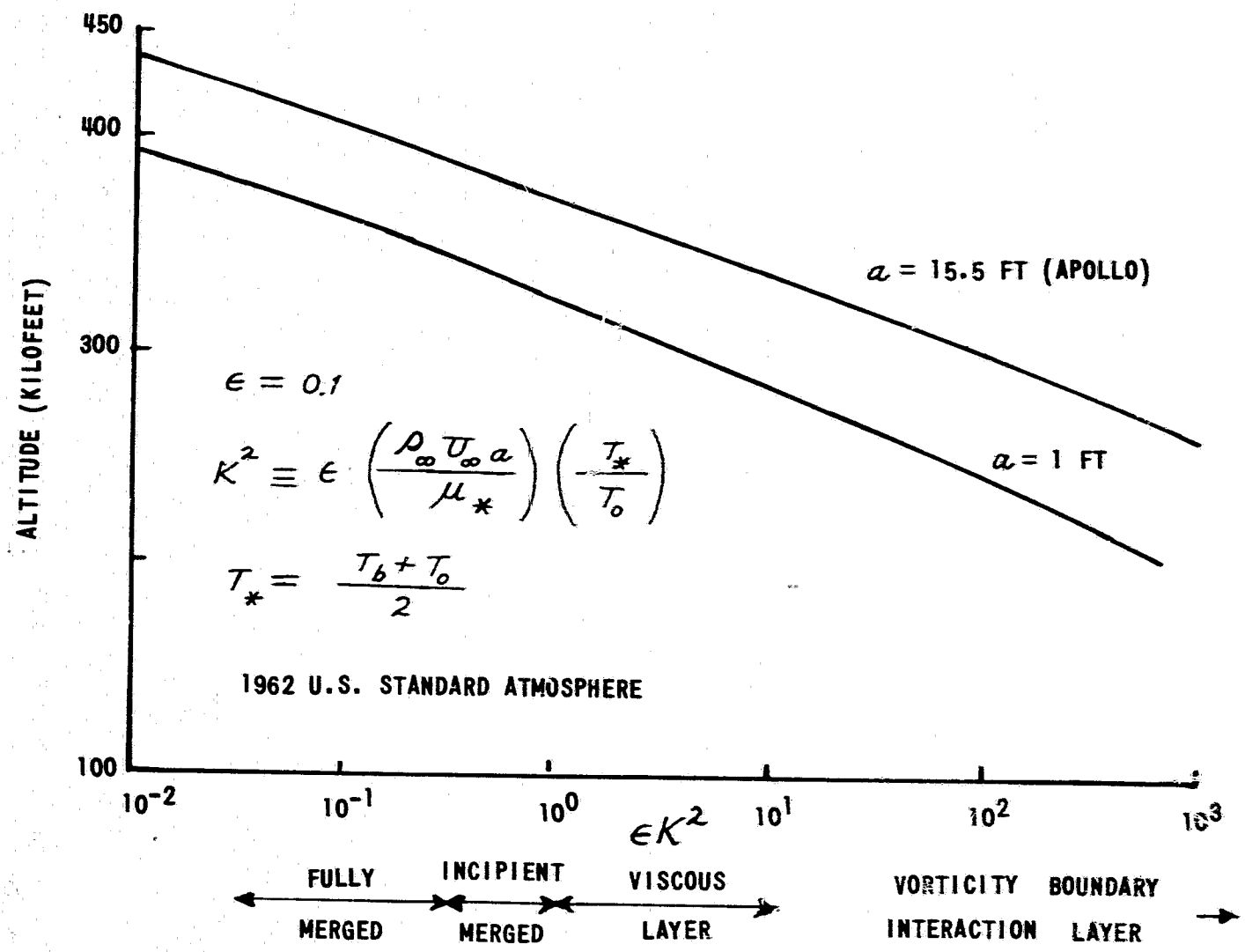

Figure 1 RAREFACTION PARAMETER AS A FUNCTION OF ALTITUDE

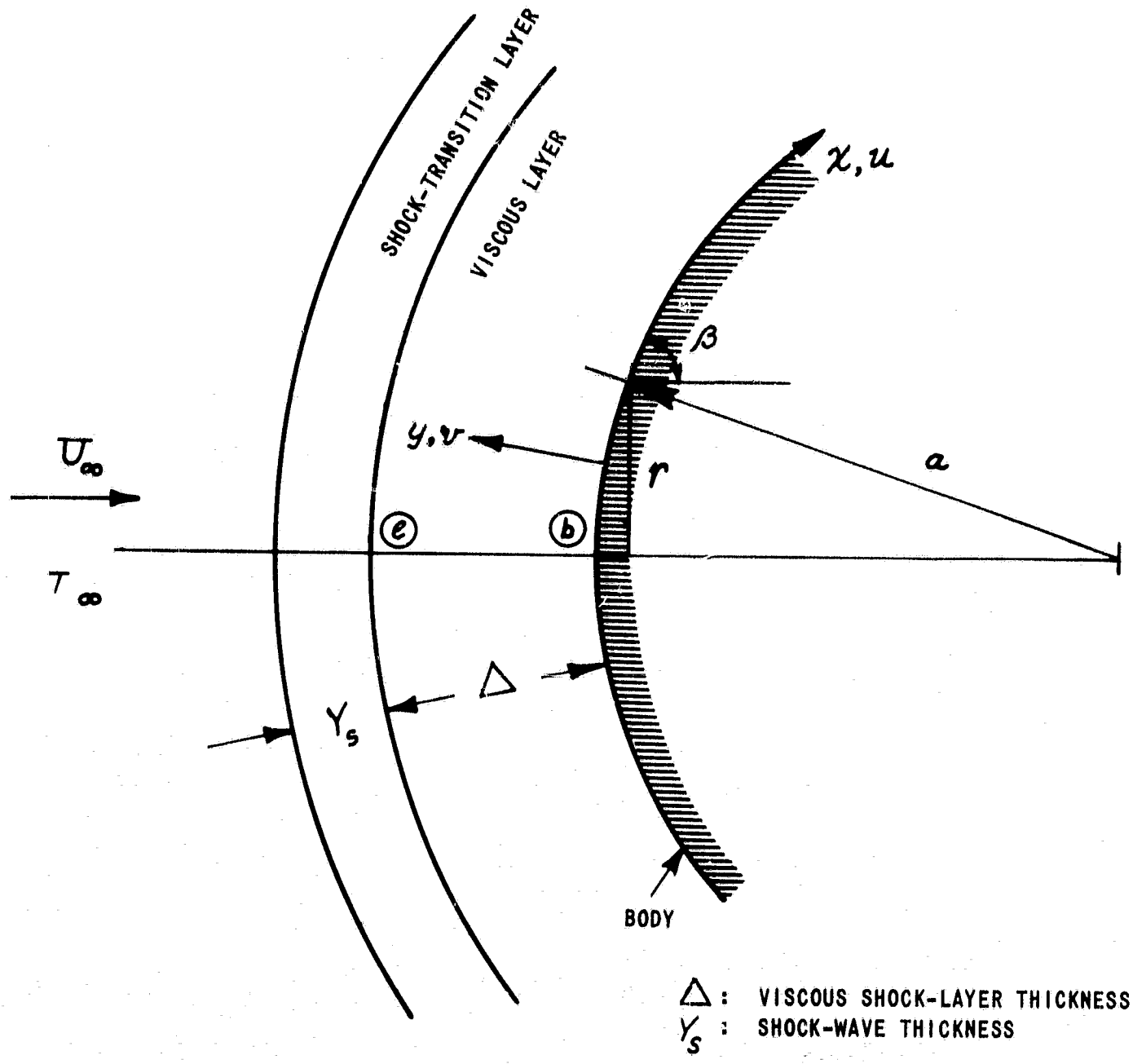

Figure 2 CO-ORDINATE SYSTEM

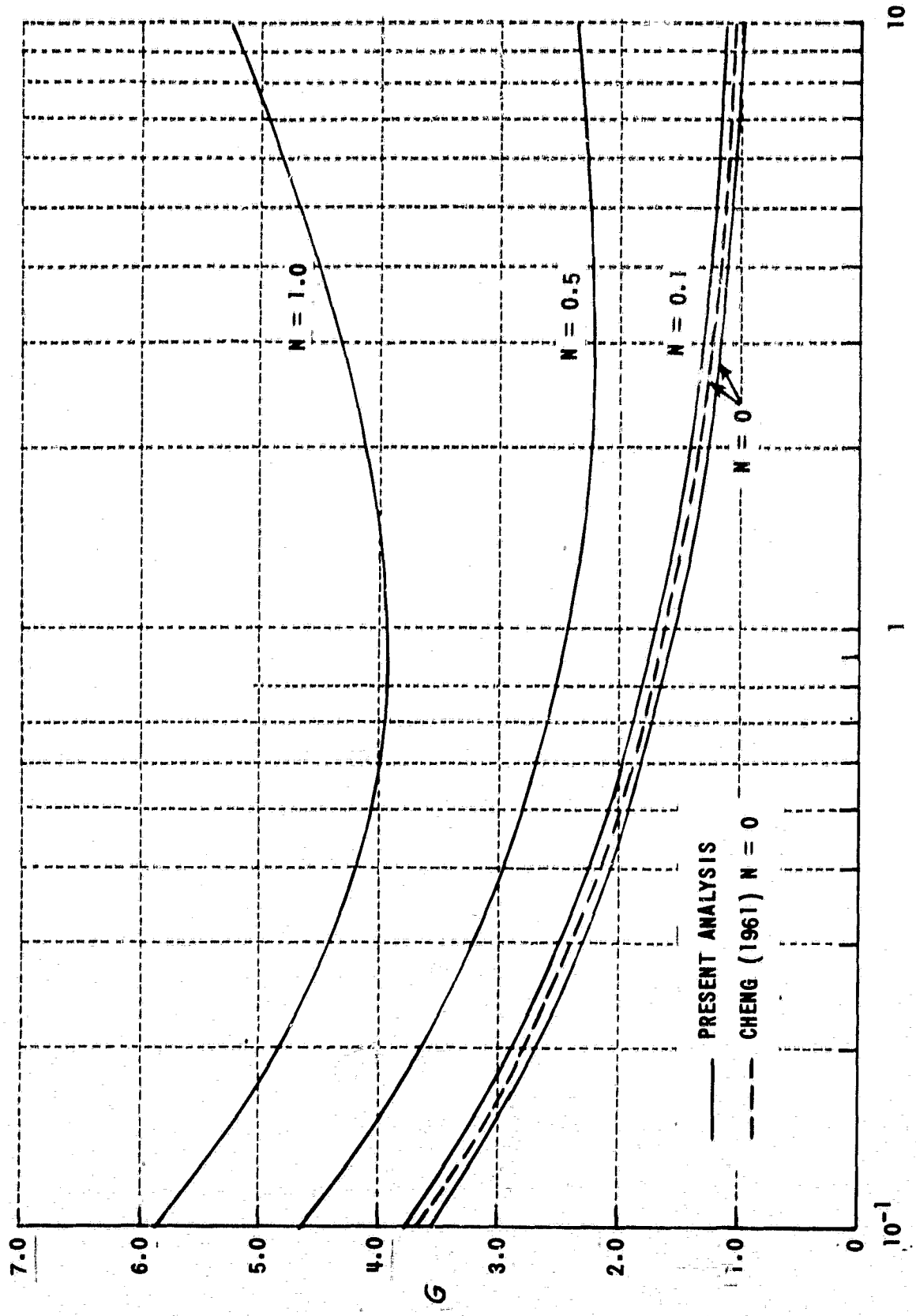

Figure 3 VALUES OF THE CHARACTERISTIC PARAMETER (G) FOR VARIOUS MASS-INJECTION RATES AT THE STAGNATION POINT AT LOW REYNOLDS NUMBER

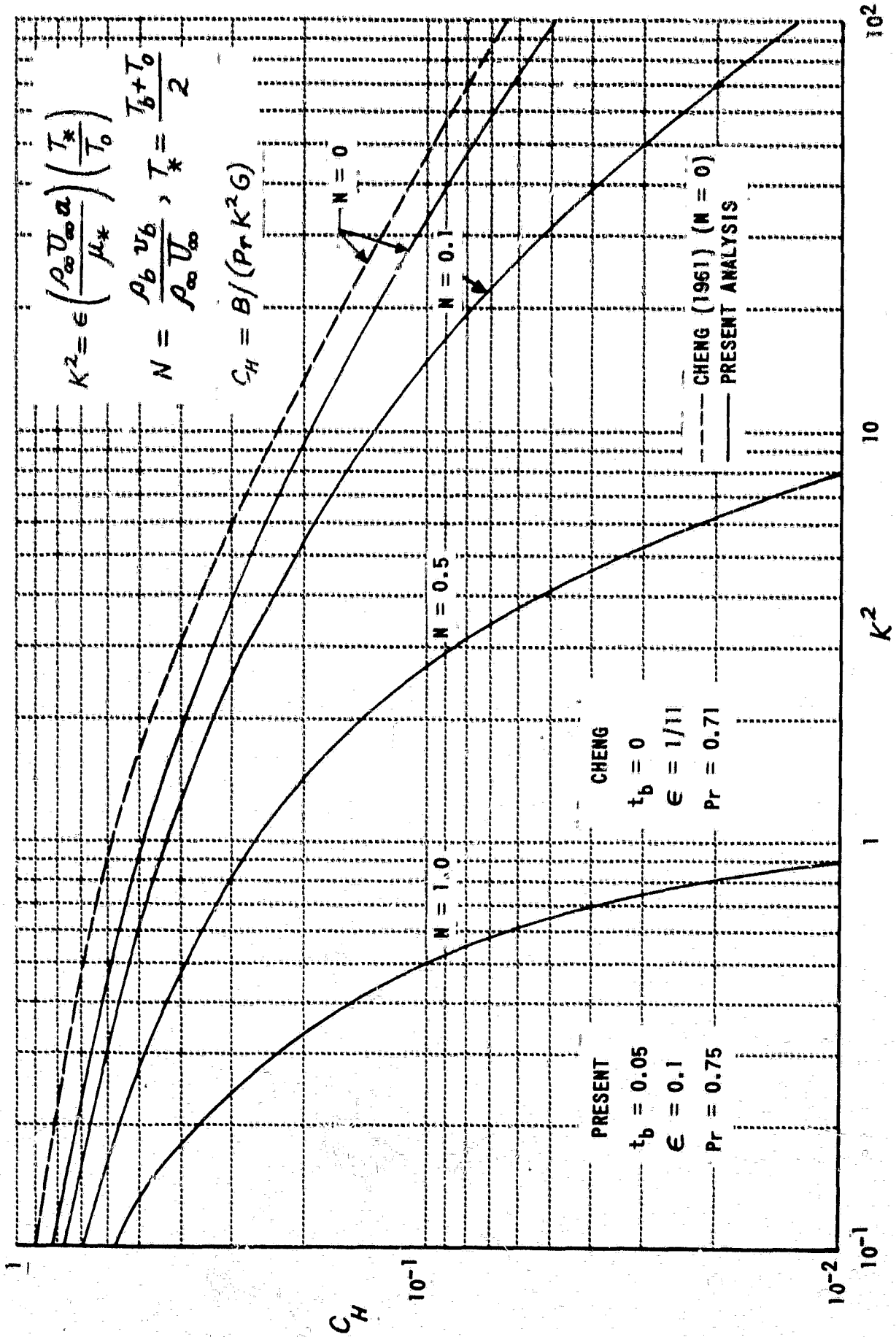

Figure 4 HEAT-TRANSFER RATES AT AN AXISYMMETRIC STAGNATION POINT FOR VARIOUS MASS-INJECTION RATES

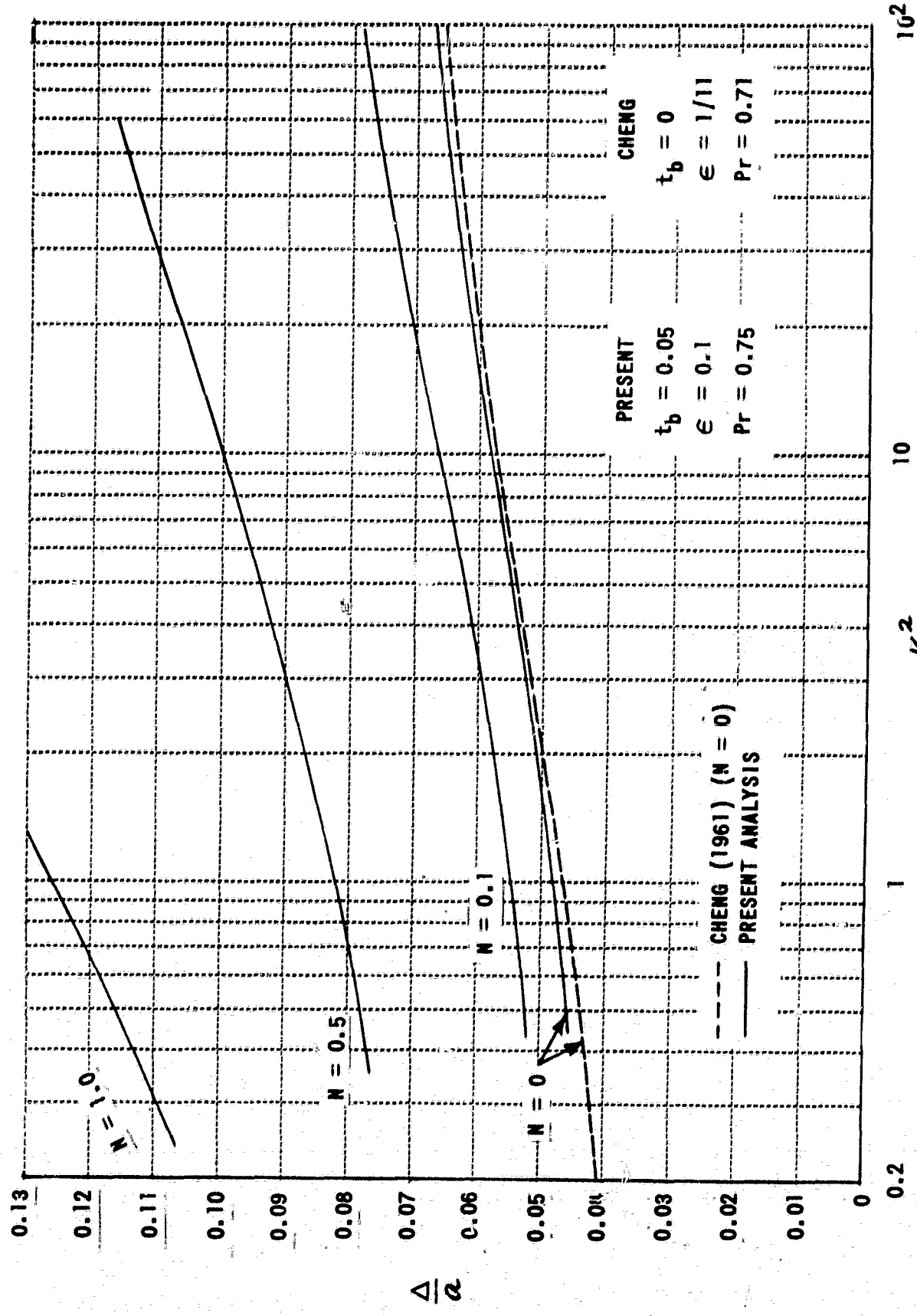

Figure 5 THE SHOCK STANDOFF DISTANCE FOR THE AXISYMMETRIC STAGNATION POINT FOR VARIOUS MASS-INJECTION RATES

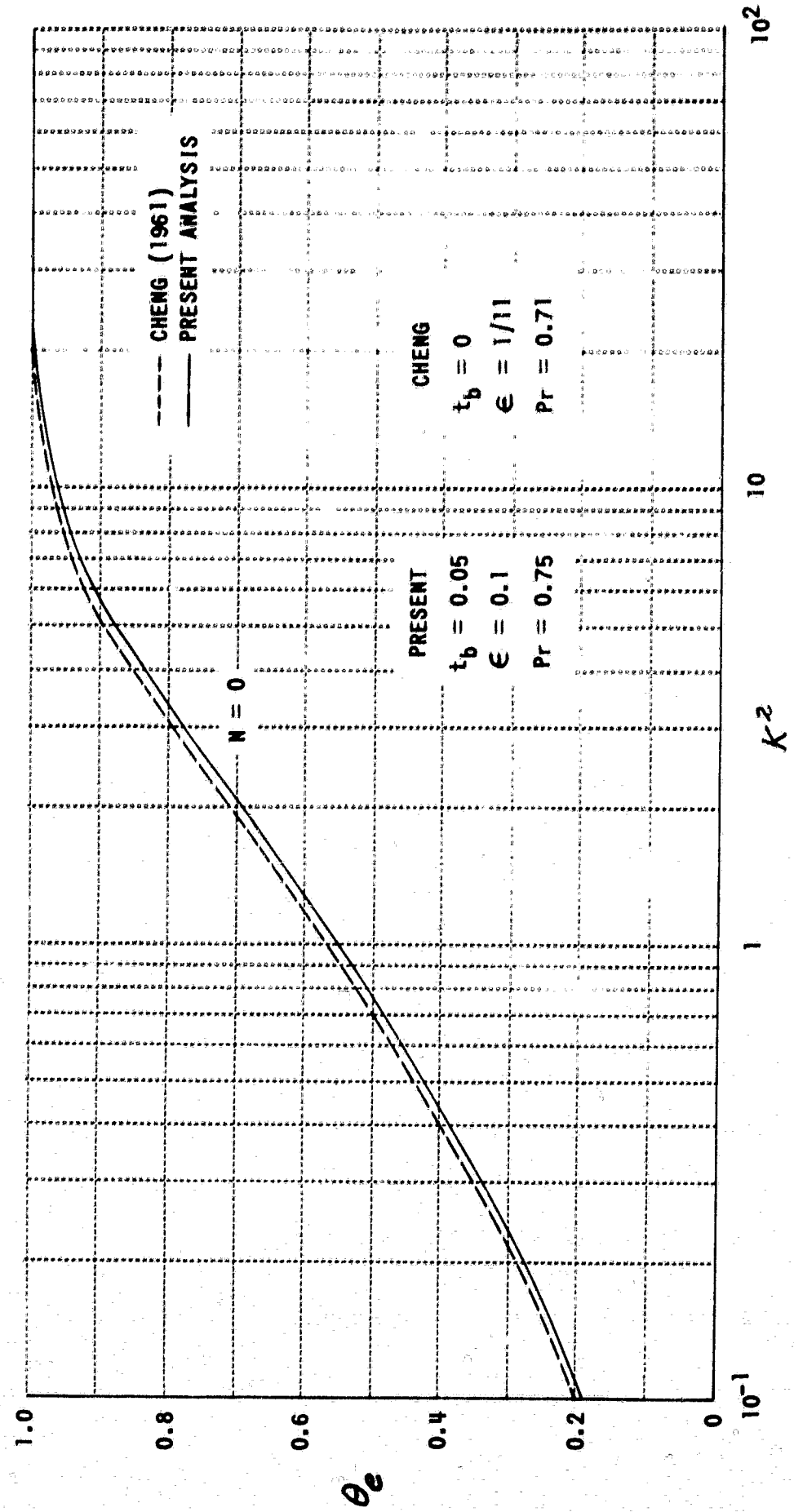

Figure 6 THE TOTAL-ENTHALPY FUNCTION IMMEDIATELY BEHIND THE SHOCK

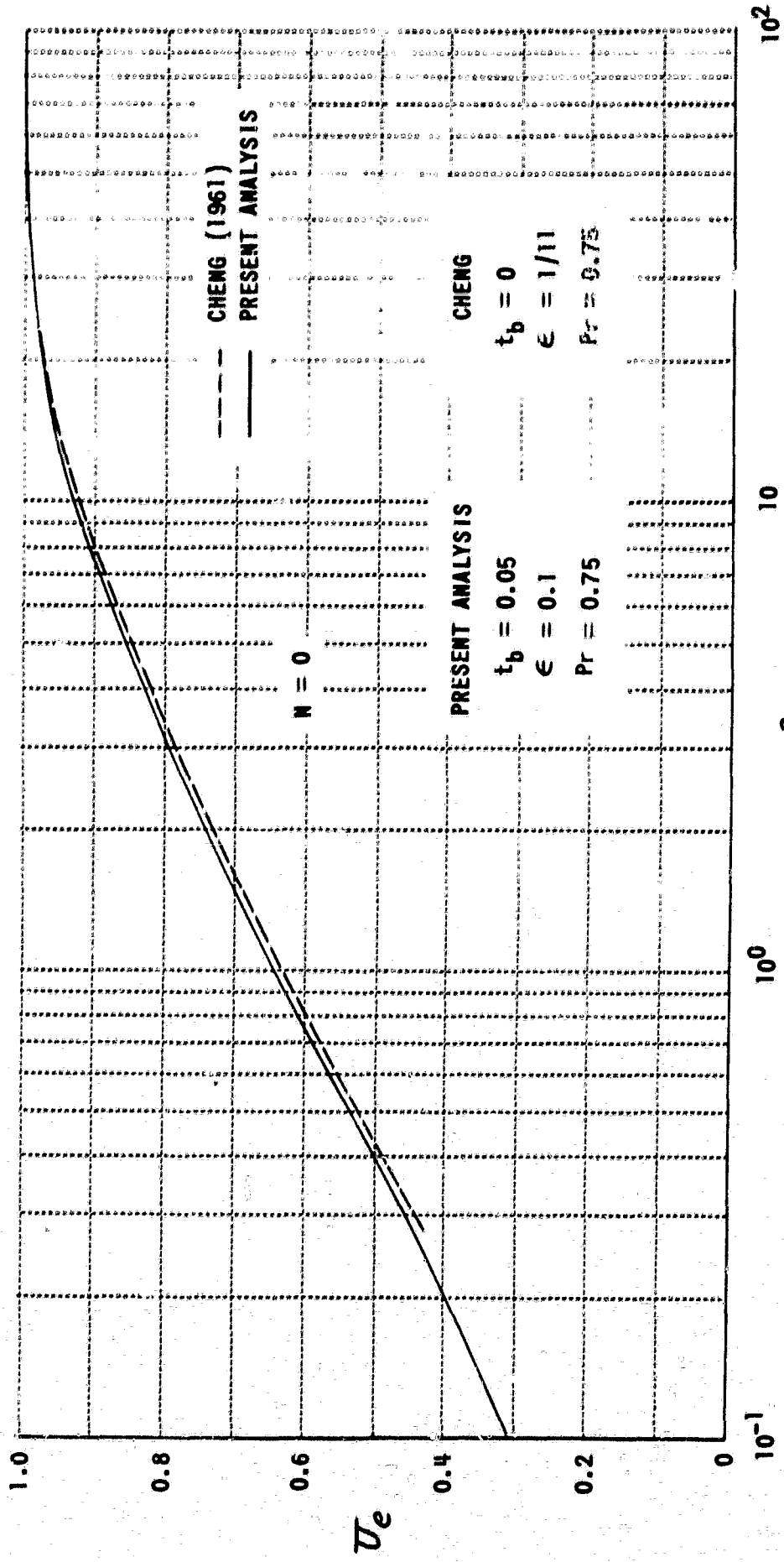

Figure 7 THE VELOCITY FUNCTION IMMEDIATELY BEHIND THE SHOCK

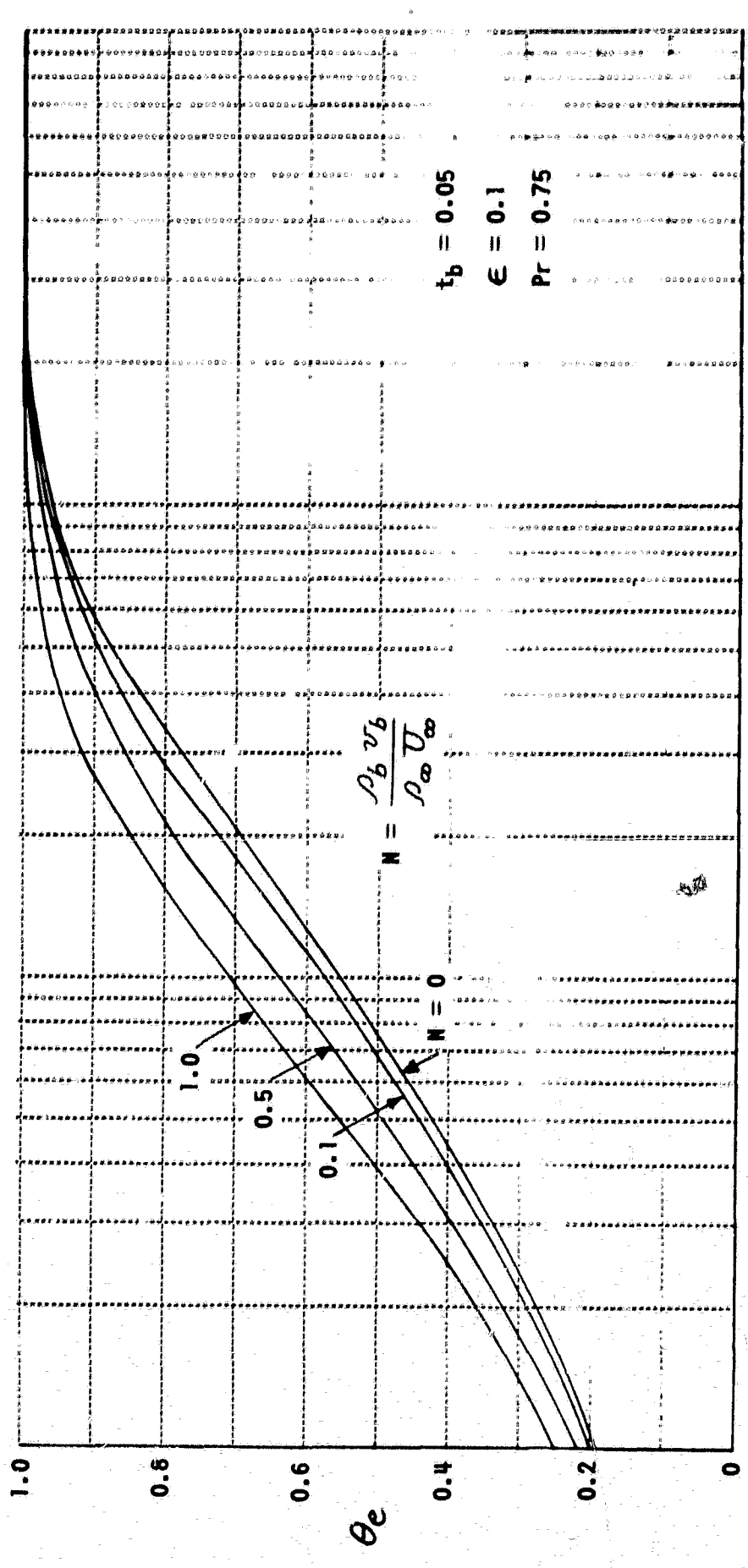

Figure 8 THE TOTAL-ENTHALPY FUNCTION IMMEDIATELY BEHIND THE SHOCK FOR VARIOUS MASS-INJECTION RATES

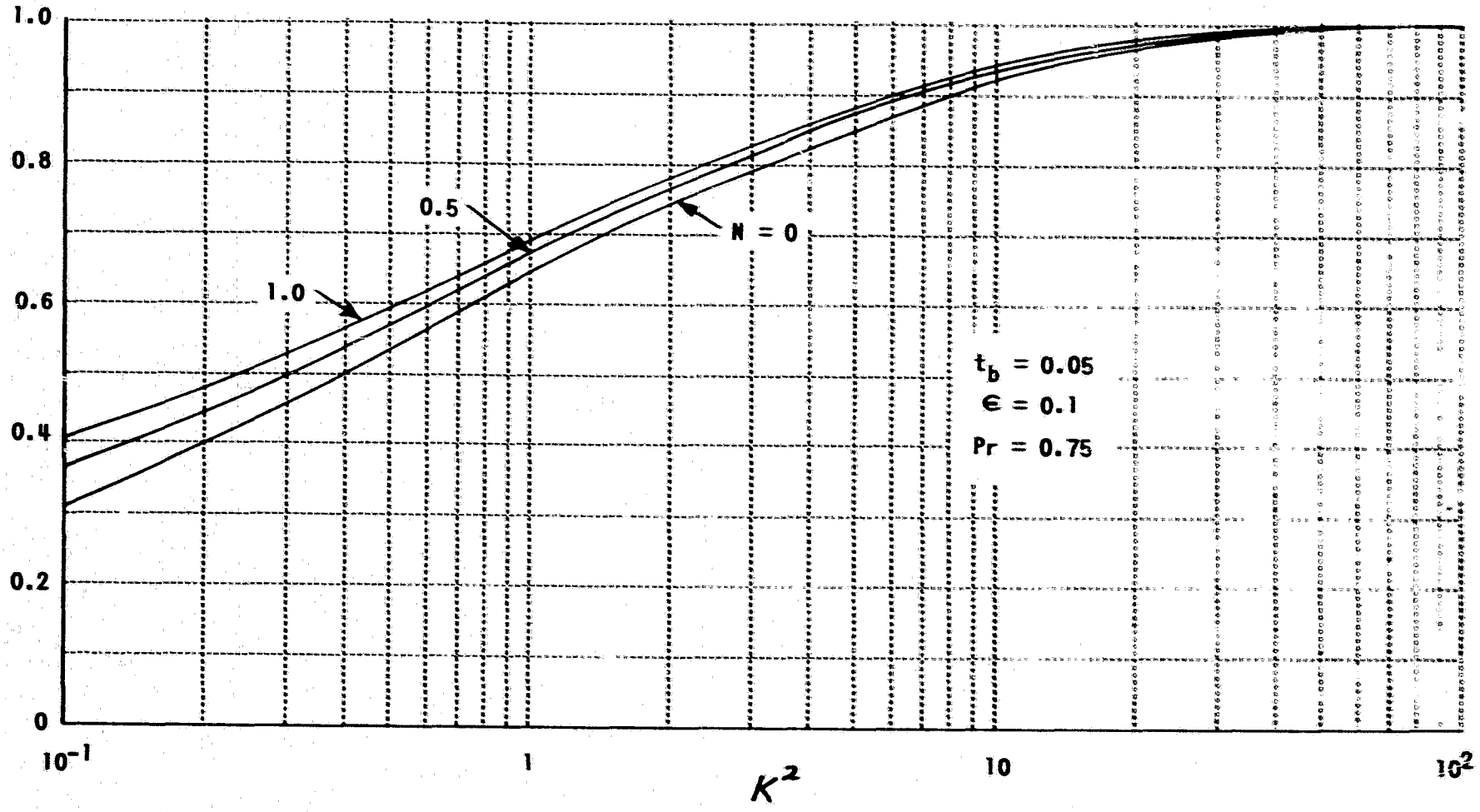

Figure 9 THE VELOCITY FUNCTION IMMEDIATELY BEHIND THE SHOCK FOR VARIOUS MASS-INJECTION RATES